Scientific Papers of the University of Pardubice, Series A; Faculty of Chemical Technology
28 (2022) 115–126.

UNIVERSITY OF PARDUBICE FACULTY OF CHEMICAL TECHNOLOGY

Advances in perovskite doping – $SrTiO_3$ with cobalt ions

Jiří Fejk*, Žaneta Dohnalová, and Pavla Honcová

Department of Inorganic Technology,
The University of Pardubice, CZ−532 10 Pardubice, Czech Republic

Received: May 25, 2022; Accepted: June 29, 2022

This paper supports the point of research on doping of inorganic materials – in this case, pigments – with various elements. Compounds on the basis of $SrTiO_3$ with individually substituted titanium positions for the cobalt ions have been prepared by the solid-state reaction boosted by the prior-to-made mechanoactivation. Calcination temperature and the molar ratio of reactants were varied in order to study their effect on the pigment synthesis. Powdered materials were characterised in terms of thermal behaviour and the phase composition. Particle size distribution and application possibilities in ceramic glaze and organic binder along with colour properties were subsequently determined for selected samples. The prepared set of pigments $SrTi_{1-x}Co_xO_3$ (x = 0.1–0.9) differed in characteristics according to a diverse range of substitution and conditions of the synthesis.

Keywords: Perovskite pigment; Black pigment; $SrTiO_3$; Cobalt; Colour properties

Introduction

Inorganic pigments have been an important part in the evolution of humans since prehistoric times. These substances can be considered as one of the chemicals that are used and produced in the greatest degree. Moreover, modern science constantly discovers new properties and ways of how to utilize these materials and so, they can be found in these days not only in cave paintings, ceramics, garments, cosmetics, typography plastics, constructions, and artistic creations but also in catalysis, environmental protection, batteries, optics, or even as so-called cooling pigments

* Corresponding author, ✉ jirka.fejk@seznam.cz

because of well obtainable solar reflectivity. Moreover, many of the previously conventional substances are not acceptable today because of their hazards to humans and nature [1–3].

One of the ways out is the synthesis of oxides of suitable metals; for example, in the perovskite structure doped with transition metals [4,5]. The general formula of the most abundant perovskite can be schematized as ABO_3 where the relatively large atom "A" holds the edges of the pseudocubic lattice, the letter "B" represents a relatively small atom in the centre, and "O" represents the oxygen atoms in the centres of the lattice sides. These compounds show various characteristics, from superconductivity or nonconductivity, via optical effects, up to electric and magnetic powers. In addition, perovskites enable easy substitution not only for transition metals, but also for almost 90 % of the elements of the periodic table. Due to a partial substitution, $A_{1-x}A'_xB_{1-y}B'_yO_3$ compounds can be prepared quite simply [6,7].

Partial or absolute substitution gives rise to changes in the oxidation states, as well as of the crystalline lattice mobility. It also forms the oxygen vacancies and other defects in the perovskite structure. The strong bond between a metal at the position of atom B and oxygen determines the elementary qualities of perovskites and also, e.g., catalytic activity. The use of various cations with different charges and diameters can thus alter all the principal properties [7,8].

Pigments are frequently made out of carbonates, oxides, nitrates, etc. by a solid-state reaction at a temperature at least 2/3 of the melting point for several hours. The disadvantages of this simple, conventional, and well-reproducible method are inhomogeneity, formation of coarser structure, and/or increased possibility of pollution due to repeated temperature and milling [7–9]. Microwave synthesis is favourable from the perspective of considerably shorter reaction time, high effectivity, and lower temperature [10]. The so-called wet-chemical synthesis allows one to create the particles of better geometrical qualities but at the cost of more demanding processes, which, among others, means advanced equipment and often dangerous reagents. For example, simple oxides can be obtained by co-precipitation of two different cations in the presence of an agent reducing the solubility [8]. Hydrothermal method produces crystalline powders out of reactions in solutions under the influence of high pressure and temperature [11] and thus cannot compete with the solid-state reaction in industrial expenses. A sol-gel method utilizes hydrolysis and polycondensation of metal alkoxides or (in the presence of water) of inorganic salts, chelation agents and/or carboxylic acids [12].

Mechanoactivation – which means high-energy ball milling in an easy and simply controlled way – leads to the formation of many structural defects that can be responsible for new properties and also reduce the required calcination temperature [13–15]. More specifically, for the synthesis of perovskite $SrTiO_3$, there is a positive influence of mechanoactivation prior to calcination confirmed by comparison of X-ray Powder Diffraction (XRD) records for reactants not treated

and high-energy ball milled. Mechanoactivated $SrCO_3$ and TiO_2 showed less intensive or even completely absent peaks in their diffractograms. Furthermore, the reaction temperature diminished from 1300 °C to 900 °C [16].

Ions Co^{2+} in positions instead of octahedral Ti^{4+} (as $SrCo_{0,3}Ti_{0,7}O_3$) enable to double the photocatalytic activity [17]. Moreover, magnetic powers can be enhanced by cobalt, as well as surface and catalytic activity. Magnetic $SrTiO_3$ can be a suitable semi-conductor in spintronics devices [18]. Properly modified perovskites seem to be possible successors to the precious metals in automotive catalytic converters. Although $SrTiO_3$ alone is not sufficiently capable of oxidizing CO molecules to CO_2, a doping with cobalt reduces the energetic barrier of absorption of CO to the surface of $SrTiO_3$ and, moreover, adds the feasibility of reducing the molecules of NO [19].

In case of pigment utilization, a strontium titanate dopped with chromium ions was studied [20]. Substitution of titanium ions by other metals is not described in the pigment concerned literature. Thus, the synthesis of perovskite $SrTiO_3$ dopped with cobalt ions was of main interest in the study presented herein.

Materials and Methods

Chemicals and Synthesis

As starting reactants, $Co(OH)_2$ (99% purity, Shepherd Color Company, Cincinnati, OH, USA), $SrCO_3$ (>99,9% purity, Sigma-Aldrich, Prague, Czech Republic) and TiO_2 (>99% purity, Precheza, Přerov, Czech Republic) were used. Reagents were mixed in the molar rations corresponding to the composition of $SrTi_{1-x}Co_xO_3$ (x = 0.1–0.9). The mixtures were manually ground in porcelain mortar and then mechanoactivated by a planetary mill Pulverisette (Fritsch, Idar-Oberstein, Germany) in agate bowls with balls of the same material (1 cm diameter) at 200 rpm for 6 hours. The obtained powders were washed with ethanol and then dried in a laboratory dryer for 20 hours. Calcination took place in corundum crucibles separately for the temperature mode of 1000 °C, 1000 + 1100 °C, 1000 + 1100 + 1200 °C. Heating rate was 5 °C·min^{-1} for the duration of 3 hours. After being cooled, the products were once more manually ground up in an agate mortar and characterized.

Characterization of Samples

The samples were evaluated with respect to their thermal stability by Differential Scanning Calorimetry (DSC, LabSys evo, Setaram, Hillsborough, NJ USA) in corundum crucibles, with argon flow of 50 cm^3 min^{-1}, heating rate of 10 °C min^{-1} and temperature varied from 25 °C to 1400 °C. Subsequently, the thermal analysis

was extended by Heat Microscopy (HM, EM-210; Hesse Instruments, Osterode am Harz, Germany) with samples forming the tablets. A heating rate was of 10 °C min^{-1} and temperature from 25 °C to 1350 °C.

The phase composition was studied by XRD analysis (Miniflex 600, Rigaku, Tokyo, Japan) equipped with a vertical goniometer θ–2θ of 15 cm, a semiconductor detector D/teX ultra and X-ray tube with copper anode CuKα (I = 15 mA, U = 40 kV) as the radiation source. The samples were measured in 2θ range from 10 to 80°, with a step of 0.02° and a stepwise scan of 10° min^{-1}.

The laser diffractometer (Mastersizer 2000/MU, Malvern Instruments, Malvern, UK) was used to measure the particle size distribution in the presence of $Na_4P_2O_7$ as a dispersant agent (m = 0,0144 g, V = 760 cm^3). Before the measurement, the samples in the amount of 0,1 g were treated for 5 minutes in ultrasonic bath with the solution of $Na_4P_2O_7$ (m = 0,006 g, V = 40 cm^3). The signal was analysed by using Mie's theory.

From the applicability and colour point of view, the samples were introduced into the medium-temperature glaze G07091 (Glazura, Dobříň, Czech Republic) in an amount of 10 wt.% and calcinated for 15 minutes at 1000 °C. Pigments were also applied into the organic matrix (dispersive acrylic binder Luxol, Akzo Nobel Coatings CZ, Opava, Czech Republic) in mass tone. The homogenized coloured matrix was deposited on the white non-absorbing glossy paper using the Bird film applicator with typical thickness of the wet film 100 μm. The colour properties of the pigment applications were measured by a spectrophotometer (UltranScan VIS, HunterLab, Reston, VA, USA) configurated to the standard illuminant and geometry $D_{65/10}$ with 9.5 mm aperture.

The colour properties were measured in the CIELAB system, and value of chroma calculated by the fallowing equation:

$$C = \sqrt{(a^*)^2 + (b^*)^2} \tag{1}$$

Results and Discussion

Thermal Analysis

As a fundamental characteristic, the thermal stability of the pigments prepared was evaluated together with verification of the temperature of 1000 °C as a sufficient heat for the reactions among the raw materials. For this analysis, the sample with the lowest substitution of titanium ions by cobalt was selected (Fig. 1).

In Figure 1, it can be seen that the sample $SrTi_{0.9}Co_{0.1}O_3$ progressively loses its mass above the temperature of 200 °C. This effect is accompanied by minor variations in enthalpy up to 1200 °C, which corresponds to the recorded noise.

In the temperature interval of 1200–1400 °C, an intensive endothermic effect with minima at 1330 °C was recorded. A sharp shape of an endothermic peak usually corresponds to the melting effect. But the peak displayed in Fig. 1 can be more possibly a result of interaction of the sample with the crucible than a process or a reaction in the sample. This hypothesis is also supported by the loss of the sample mass, which was detected by ThermoGravimetry (TG). In addition, the end of the analysis shows the change in colour of the corundum crucible surface from white to blue. This supports the assumption about the reaction of cobalt ions with the corundum crucibles leading to formation of blue spinel $CoAl_2O_4$.

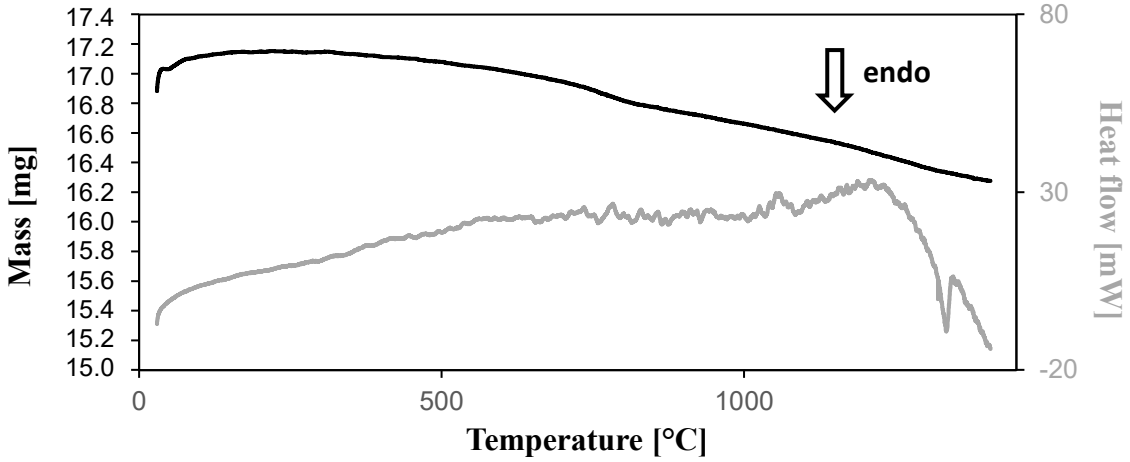

Fig. 1 DSC/TG analysis of $SrTi_{0.9}Co_{0.1}O_3$

The presumed interaction between the cobalt ions and corundum crucible during DSC demanded to examine the thermal stability of the sample by heating microscopy. For this, the samples $SrTi_{0.9}Co_{0.1}O_3$ and $SrTi_{0.1}Co_{0.9}O_3$ were investigated (Fig. 2). The sample with a higher content of doped cobalt ions was also investigated to determine the effect of the substitution range on the thermal stability of the samples.

The initial softening of the $SrTi_{1-x}Co_xO_3$ pigments is related to the extension of the area of the tablets (max. 2 %), but the samples show thermal stability up to 1072 °C (Fig. 2). Afterwards, the sintering and shrinking effects of the tablets follow. These processes are faster for the sample with a lower content of cobalt. However, an initial decrease in volume occurs first for $SrTi_{0.1}Co_{0.9}O_3$. At the end of the measurement at a temperature of 1346 °C the final areas of the tablets $SrTi_{0.9}Co_{0.1}O_3$ and $SrTi_{0.1}Co_{0.9}O_3$ are reduced to 58.4 % and 65.7 %.

No marked effect was observed when increasing the substitution range of the thermal stability of the pigments. Therefore, it can be concluded that the extent of substitution does not affect the thermal stability of the prepared pigments and that the endothermic effect with a minimum at 1345 °C detected upon the DSC curve corresponds also to the partial melting of the pigment.

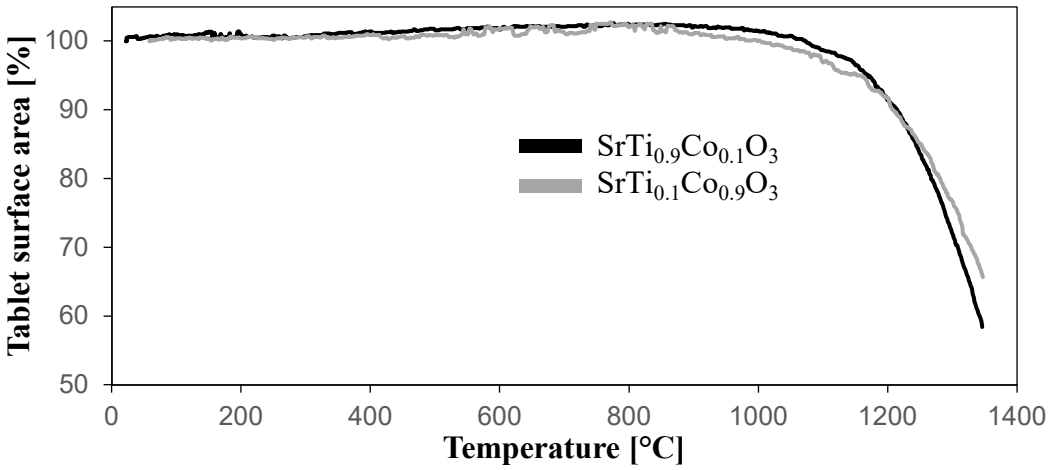

Fig. 2 Heat microscopy of $SrTi_{0.9}Co_{0.1}O_3$ and $SrTi_{0.1}Co_{0.9}O_3$

Phase composition

The phase composition of all the samples was characterised by XRD. For the synthetized $SrTi_{1-x}Co_xO_3$ powders, one could observe a significant dependency of their phase composition on the amount of the introduced cobalt ions. The respective results are summarised in Tab. 1.

Table 1 Phase composition of $SrTi_{1-x}Co_xO_3$

Range of the substitution x								
0.1	0.2	0.3	0.4	0.5	0.6	0.7	0.8	0.9
Calcination temperature: 1000 °C								
$SrTiO_3$	$SrTiO_3$	$SrTiO_3$ $SrCoO_3$	$SrTiO_3$ $SrCoO_3$	$SrTiO_3$ $SrCoO_3$	$SrTiO_3$ $SrCoO_3$	$SrTiO_3$ Sr_2CoO_4 $Sr_3Co_2O_6$ Co_3O_4	$SrCoO_3$ Sr_2TiO_4 $SrCO_3$ Co_3O_4	$SrCoO_3$ $Sr_3Co_2O_6$ $Sr_5Co_4O_{12}$ $Sr_6Co_5O_{15}$ Co_3O_4 Ti_5O_9
Calcination temperature: 1100 °C								
$SrTiO_3$	$SrTiO_3$	$SrCoO_3$ $SrTi_{0.7}Co_{0.3}O_3$	$SrTiO_3$ $SrCoO_3$	$SrTiO_3$ $SrCoO_3$	$SrCoO_3$ $SrTi_{0.7}Co_{0.3}O_3$	$SrTiO_3$ $SrCoO_3$ $Sr_3Co_2O_6$	$SrTiO_3$ $Sr_3Co_2O_6$ Sr_2TiO_4	$SrCoO_3$ $Sr_3Co_2O_6$ $Sr_6Co_5O_{15}$
Calcination temperature: 1200 °C								
$SrTiO_3$	$SrTiO_3$	$SrCoO_3$ $SrTi_{0.7}Co_{0.3}O_3$	$SrTiO_3$ $SrCoO_3$	$SrTiO_3$ $SrCoO_{2.5}$	$SrCoO_3$ $SrTi_{0.7}Co_{0.3}O_3$	$SrTiO_3$ $SrCoO_3$	$SrCoO_3$ $Sr_3Co_2O_6$	$SrCoO_3$

The samples with cobalt substitution of 10 and 20 wt.% form a single-phase system of $SrTiO_3$ regardless of the temperature mode. This indicates full-scale incorporation of dopant ions to the perovskite lattice. The pigments for the substitution range of $x = 0.3$ to $x = 0.6$ and calcination temperatures of 1000 and 1100 °C have a two-phase composition. If the heating temperature reaches 1200 °C the system will remain in two phases until $x = 0.8$. The chemical composition corresponds mostly to $SrTiO_3$ and $SrCoO_3$, but interstitial $SrTi_{0.7}Co_{0.3}O_3$ is also identified. Composition of three and more phases is obtained for $x \geq 0.7$ and calcination temperatures of 1000 °C or 1100 °C. In case of the sample, $x = 0.9$ and the temperature 1000 °C, six different compounds are identified. Besides $SrTiO_3$ and mixed strontium-cobalt oxides, also other oxides (Co_3O_4, Ti_5O_6) can be found for some of these samples. The single-phase system based on the structure of $SrCoO_3$ was obtained in the case of sample $SrTi_{0.1}Co_{0.9}O_3$ calcinated at the temperature of 1200 °C.

Fig. 3 represents the diffractograms of $SrTi_{0.9}Co_{0.1}O_3$ synthetized in all temperature modes studied. As seen, the changes in positions of all peaks are insignificant. Thus, the composition of the pigment phase does not change in accordance with the diverse temperature modes. Only the intensities of the peaks increase in correlation with higher temperature. It also supports the assessment that the temperature of 1000 °C is sufficient for the proper realization of reactions.

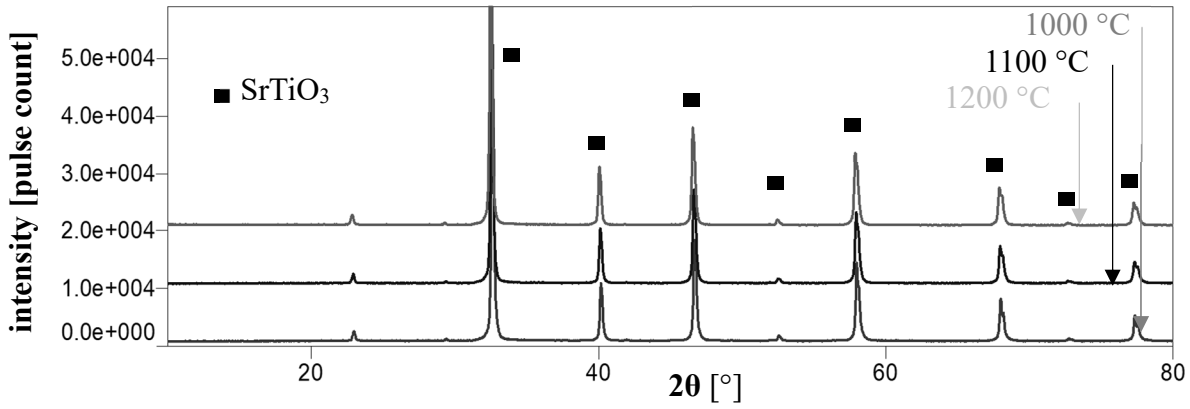

Fig. 3 XRD analysis of $SrTi_{0.9}Co_{0.1}O_3$ – all temperature mods

The improvement of phase composition by calcination temperature is obvious in Fig. 4, which represents samples with maxima of incorporated cobalt ions – $SrTi_{0.1}Co_{0.9}O_3$. The corresponding diffractograms are smoother the higher the temperature. It means that the raise in the calcination temperature supports the formation of perovskite phase.

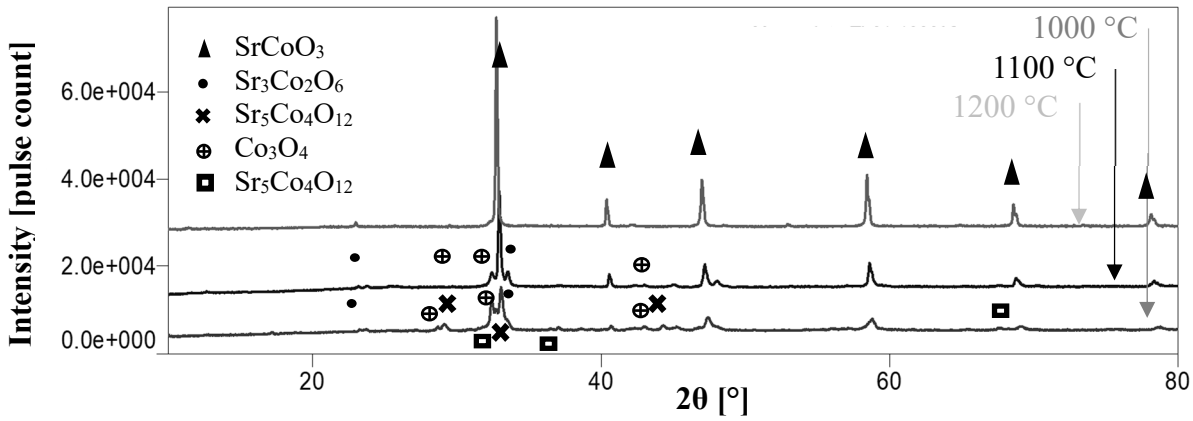

Fig. 4 XRD analysis of $SrTi_{0.1}Co_{0.9}O_3$ – all temperature mods

Particle size distribution

Both the substitution range and the calcining temperature affect the particle diameters of the $SrTi_{1-x}Co_xO_3$ pigments. As shown in Table 2, the particle size distribution is usually shifted to higher values with increasing substitution range. The quantile d_{50} increases in values from 1.4 to 2.8 μm in the case of calcination at 1000 °C; from 1.8 to 3.5 μm for the 1100°C mode and from 1.9 to 14.7 μm for 1200 °C temperature. The particles of the $SrTi_{0.1}Co_{0.9}O_3$ samples are considerably larger at all calcination temperatures.

The effect of calcination temperature exhibits the same trend, which means that the more intensive heat forms the larger particle size, both inducing and boosting the formation of agglomerates.

Table 2 Particle size distribution of $SrTi_{1-x}Co_xO_3$

	Range of the substitution *x*								
	0.1	0.2	0.3	0.4	0.5	0.6	0.7	0.8	0.9
[μm]	Calcination temperature: 1000 °C								
d (0.1)	0.5	0.6	0.7	0.9	0.9	0.9	1.0	1.0	0.9
d (0.5)	1.4	1.5	1.8	2.0	1.9	2.1	2.5	2.8	2.7
d (0.9)	3.3	3.3	7.1	10.8	19.8	21.0	20.6	31.6	24.3
[μm]	Calcination temperature: 1100 °C								
d (0.1)	0.5	0.8	1.0	1.0	1.2	1.3	1.5	1.0	0.9
d (0.5)	1.8	2.4	2.4	2.3	2.5	3.0	3.6	2.9	3.5
d (0.9)	10.8	8.3	8.2	6.8	12.2	25.1	20.4	13.4	21.4
[μm]	Calcination temperature: 1200 °C								
d (0.1)	0.7	0.8	1.0	1.0	1.1	1.2	1.4	1.8	2.8
d (0.5)	1.9	2.3	2.6	2.9	3.0	4.1	4.9	5.1	14.7
d (0.9)	16.0	12.6	14.9	15.2	15.2	37.1	40.9	31.7	65.1

Application abilities and colour properties

All prepared $SrTi_{1-x}Co_xO_3$ pigments formed very similar black powders without the possibility to subjectively distinguish its shades by an eye.

Despite the thermal stability of the samples which was established as that withstanding the temperatures above 1070 °C, synthetized pigments were not suitable for application in glazes. After calcination, the colouration of the glaze was unequal, and the surface disrupted by bubbles and cracks. The cause of the defects has been attributed to the low chemical stability of the samples of molten glass. Fig. 5 represents a black-and-white photograph of selected samples applied into the ceramic glaze G07091 and calcined at 1000 °C for 15 min.

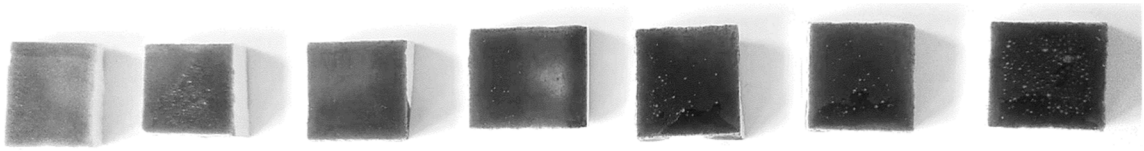

Fig. 5 Photo (adjusted to highlight the flaws) of pigment $SrTi_{1-x}Co_xO_3$ application into the glaze G07091 (1000 °C, 15 min)

The application of pigments prepared into the organic matrix was successful for almost all samples. The coarseness of the $SrTi_{1-x}Co_xO_3$ samples increased with higher substitution range, causing impossibility of creating a proper coloured film. This observation holds true for sample $x = 0.9$ in all temperature mods. In the case of calcination at 1200 °C, the negative effect of coarseness can be observed for samples with $x \geq 0.7$. Therefore, both the temperature and amount of cobalt affect the product's application properties.

From the colour point of view, all the $SrTi_{1-x}Co_xO_3$ samples applied into organic matrix were also subjectively indistinguishable by the naked eye.

As can be seen in Table 3, a raise of the calcination temperature from 1100 to 1200 °C slightly increases the lightness of the applied samples (L^*). It also shifts the coordinate b^* toward lower values (except of $x = 0.8$) and almost does not affect the coordinate a^*. The pigment with $x = 0.1$ is deviates noticeably from other samples. The sample with $x = 0.1$ calcinated at 1100 °C has exhibited the highest values of all parameters, namely: $L^* = 28.7$; $a^* = 1.18$; $b^* = 1.26$ and $C = 1.73$. Thus, the sample $SrTi_{0.1}Co_{0.9}O_3$ was lighter than the others. Its a^* and b^* parameters place this sample to red and yellow field of the CIELAB system. The values of the other powders fall into a green-blue region. However, due to the low values of the colour parameters a^* and b^*, the resulting colour of all samples was black. That has implied that the most beneficial values of a^*, b^* and C are the lowest (centre of the colour system) for the black pigments. This desired positive shift could be clearly obtained by adding of more cobalt ions and/or by calcination at the temperature of 1200 °C (Table 3).

The highlighted areas are given in Table 3. The best black colour coordinates was reached by the amount of cobalt with $x = 0.8$. This means that these samples have values of a^* and b^* close to the origin of CIELAB coordinates. The lowest values of lightness and almost the most intensive saturation were obtained for samples with $x = 0.3$ and $x = 0.4$. They are not as black as the more substituted samples, but they are shifted mainly to the blue region (negative b^*) of the colour system. As a result, this property can appear to be favourable for perception of black colour.

Table 3 Colour coordinates (CIELAB) of $SrTi_{1-x}Co_xO_3$ applied into the organic matrix

	Range of the substitution x								
	0.1	0.2	0.3	0.4	0.5	0.6	0.7	0.8	0.9
	Calcination temperature: 1000 °C								
L^*	28.7	24.8	24.5	23.9	25.7	25.3	25.1	26.5	–
a^*	1.18	0.08	–0.18	–0.23	–0.21	–0.21	–0.19	–0.17	–
b^*	1.26	–0.85	–1.12	–0.97	–0.80	–0.57	–0.25	–0.21	–
C	1.73	0.85	1.13	1.00	0.83	0.61	0.31	0.27	–
	Calcination temperature: 1200 °C								
L^*	28.0	26.3	25.5	25.8	26.0	26.5	27.0	26.2	–
a^*	0.68	–0.08	–0.20	–0.23	–0.23	–0.23	–0.21	–0.24	–
b^*	0.31	–0.82	–0.86	–0.77	–0.59	–0.32	0,13	0,24	–
C	0.75	0.82	0.88	0.80	0.63	0.39	0.25	0.34	–

Conclusions

In this article, out new research is presented focused on the synthesis and characterisation of new inorganic pigments on the base of $SrTiO_3$ substituted by cobalt in the titanium positions. The influence of the substitution range and the calcination temperature on the properties of the pigments has been investigated. As ascertained, the phase composition of the $SrTi_{1-x}Co_xO_3$ samples was affected the most significantly. The single-phase products were synthetized in compositions $SrTi_{0.9}Co_{0.1}O_3$, $SrTi_{0.8}Co_{0.2}O_3$ (for all calcination mods) and $SrTi_{0.1}Co_{0.9}O_3$ (for a temperature of 1200 °C).

Despite the determined thermal stability, the synthetized black pigments were found unsuitable for application into ceramic glazes due to their chemical instability. However, prepared black powders are suitable for application in an organic matrix. Regarding the phase composition, CIELAB parameters, colour perception and application properties, the sample $SrTi_{1-x}Co_xO_3$ with 30 % of cobalt and calcined up to 1200 °C seems to be the optimal one.

Acknowledgment

This research has been supported by the University of Pardubice under the project SGS_2022_007.

References

[1] Sheethu J., Deepak J., Soumya B.N., Periyat P.: Recent advances in infrared reflective inorganic pigments. *Solar Energy Materials and Solar Cells* **194** (2019) 7–27.

[2] Gramm G., Fugrmann G., Wieser M., Schottenberger H.: Environmentally benign inorganic red pigments based on tetragonal beta-Bi_2O_3. *Dyes and Pigments* **160** (2019) 9–15.

[3] Serment B, Corucho L., Demourgues A., Hadziioannou G., Brochon C., Cloutet E., Gaudon M.: Tailoring the chemical composition of $LiMPO_4$ (M = Mg, Co, Ni) orthophosphates to design new inorganic pigments from magenta to yellow hue. *Inorganic* **58** (2019) 7499–7510.

[4] Yuan L., Han A., Ye M., Chen X., Yao L., Ding C.: Synthesis and characterization of environmentally benign inorganic pigments with high NIR reflectance: Lanthanum-doped $BiFeO_3$. *Dyes and Pigments* **148** (2018) 137–146.

[5] Li J., Subramanian M.A.: Inorganic pigments with transition metal chromophores at trigonal bipyramidal coordination: $Y(In,Mn)O_3$ blues and beyond. *Journal of Solid State Chemistry* **272** (2019) 9–20.

[6] Luxova J., Šulcová P., Trojan M. Study of perovskite compounds. *Journal of Thermal Analysis and Calorimetry* **93** (2008) 823–827.

[7] Atta N.F., Gala A., Ekram E.: Perovskite nanoamterials – synthesis, characterization, and applications. *Perovskite Materials: Synthesis, Characterisation, Properties, and Applications.* InTech, Rijeka, 2016, pp. 107–136.

[8] Assirey E.A.R.: Perovskite synthesis, properties and their related biochemical and industrial application. *Saudi Pharmaceutical Journal* **27** (2019) 817–829.

[9] Tsukimori T., Oka R., Masaui T.: Synthesis and characterization of $Bi_4Zr_3O_{12}$ as an environment-friendly inorganic yellow pigment. *Dyes and Pigments* **139** (2017) 808–811.

[10] Menon S.G., Swart H.C.: Microwave-assisted synthesis of blue-green $NiAl_2O_4$ nanoparticle pigments with high near-infrared reflectance for indoor cooling. *Journal of Alloys and Compounds* **819** (2020) 1–7.

[10] Calatayud J.M., Alarcón J.: V-containing ZrO_2 inorganic yellow nano-pigments prepared by hydrothermal approach. *Dyes and Pigments* **146** (2017) 178–188

[12] Bakhshi H., Sarraf-Mamoory R., Yourdkhani A., AbdelNabi A.A., Mozharivskyj Y.: Sol-gel synthesis, spark plasma sintering, structural characterization, and thermal conductivity measurement of heavily Nb-doped $SrTiO_3/TiO_2$ nanocomposites. *Ceramics International* **46** (2020) 3224–3235.

[13] Gerasimova L.G., Maslova M.V., Shchukina E.S. : Role of mechanoactivation in preparation of mineral filler pigment from titanite. *Russian Journal of Applied Chemistry* **83** (2010) 2081–2087.

[14] Wang M., Woo K., Lee C.: Preparing $La_{0.8}Sr_{0.2}MnO_3$ conductive perovskite via optimal processes: High-energy ball milling and calcinations. *Energy Conversion and Management* **52** (2011) 1589–1592.

[15] Piotr D.: *Solid-state mechanochemical syntheses of perovskites.* InTech, Rijeka, 2016, pp 4–21.

[16] Parlak T.T., Apaydin F. Yildiz K.: Formation of $SrTiO_3$ in mechanically activated $SrCO_3$–TiO_2 system. *Journal of Thermal Analysis and Calorimetry* **127** (2017) 63–69.

[17] Ichihara F., Murata Y., Ono H., Choo C., Tanaka K.: Characterization of $SrTiO_3$ target doped with Co ions, $SrCo_xTi_{1-x}O_{3-\delta}$, and their thin films prepared by pulsed laser ablation (PLA) in water for visible light response. *Applied Surface Science* **419** (2017) 126–137.

[18] Sluchinskaya I., Lebedev A.I.: Electronic and magnetic properties of structural defects in $SrTiO_3$(Co). *Journal of Alloys and Compounds* **820** (2020)

[19] Carlotto S., Natile M.M., Glisenti A., Paul J., Blanck D., Vittadini A.: Energetics of CO oxidation on lanthanide-free perovskite systems: the case of Co-doped $SrTiO_3$. *Physical Chemistry Chemical Physics* **18** (2016) 33282–33286.

[20] Yongvanich, N., Srithog, K; Kaewbudsa, W.; Visuttipitukul, P.: New Cr-doped $SrTiO_3$ ceramic color pigment. *Applied Mechanics and Materials* **709** (2014) 346–349.